Engineering Structures 179 (2019) 321–331

Contents lists available at ScienceDirect

Engineering Structures

journal homepage: www.elsevier.com/locate/engstruct

3D aerodynamic admittances of streamlined box bridge decks☆

Cunming Ma[a,*], Junxin Wang[a], Q.S. Li[b,*], Haili Liao[c]

[a] School of Civil Engineering, Southwest Jiaotong University, Chengdu 610031, China
[b] Department of Architecture and Civil Engineering, City University of Hong Kong, Hong Kong
[c] Key Laboratory for Wind Engineering of Sichuan Province, Chengdu 610031, PR China

ARTICLE INFO

Keywords:
Aerodynamic admittance
Bridge decks
Aerodynamic force
Wind tunnel test

ABSTRACT

Via wind tunnel tests, the fluctuating pressures on the surfaces of three streamlined box bridge models are measured in two turbulent flow-fields with different turbulence characteristic parameters. The distributions of the fluctuating pressures on the models are presented and discussed in detail. The correlations between the fluctuating pressures on a crosswise section and the coherences of the buffeting force along the spanwise direction of the models are investigated. Furthermore, the 3D aerodynamic admittances of the models are identified and analyzed. An empirical formula for determining the 3D aerodynamic admittance of a streamlined bridge deck is proposed based on the extensive results of the experimental data and analysis. Clarifications are made regarding the differences between the real 3D aerodynamic admittances and the existing formulas. It is then further revealed that the real value of a 3D aerodynamic admittance is not between 1 and the number determined by the Sears function. This is followed by a rational explanation for the observations based on the experimental results.

1. Introduction

Aerodynamic admittance is a transformation function that depicts the relationship between the incident turbulent wind velocity and the fluctuating wind load acting on a structure, and is a key aerodynamic parameter in estimating the structural responses of long-span bridges. The earliest studies of aerodynamic admittance were carried out as part of aerodynamics research in the 1930s [1]. The Sears function was theoretically derived as the aerodynamic admittance function of a airfoil, which is also referred to as a flat plate. It is given by Sears [2]:

$$\chi^2(f) = \frac{J_0(\widetilde{k})K_1(i\widetilde{k}) + iJ_1(\widetilde{k})K_0(i\widetilde{k})}{K_1(i\widetilde{k}) + K_0(i\widetilde{k})} \tag{1a}$$

where $\widetilde{k} = f\pi B/U$ is a non-dimensional parameter, f is the wind fluctuation frequency, B is the airfoil width, U is the mean wind velocity, J_0 and J_1 are Bessel functions of the first kind and K_0 and K_1 are modified Bessel functions of the second kind. The Sears function may be approximated by a simple expression suggested by Liepmann [3]:

$$|\chi(f)|^2 = \frac{1}{1 + 2\pi\widetilde{k}} \tag{1b}$$

The assumptions involved in Sears function include (i) the strip assumption (i.e., that the fluctuating wind speed correlates fully along the spanwise direction and ignores the spatially correlative characteristics of turbulence); (ii) that the characteristic size of the structure concerned is small enough in comparison with the turbulence length scale of the incident wind velocity; (iii) that there is no separation of the shear layers and full coherence of the fluctuating pressures along the section width of the whole structure. In fact, these assumptions do not strictly apply to bridge decks for to the following reasons:

- For the buffeting lift force and moment, the characteristic length of a bridge is the width of the deck, namely B. The width of the deck is not small enough in comparison with the turbulence length scale and flow reattachment may occur accordingly. In this situation, the fluctuating pressures on a crosswise section are not fully correlated.
- The buffeting forces on different sections along the spanwise direction may influence each other because of the spatially correlative characteristics of turbulence in the atmosphere, which do not satisfy the “strip assumption”.
- Bridge decks are bluff bodies with different geometrical shapes. In fact, the interaction between a structure and incident fluctuating winds is complicated, and no theoretical formulation is available to deal with such a problem for bluff bodies like bridge decks.

☆ The work described in this paper was fully supported by grants from the National Natural Science Foundation of China (Project No. 51778545).
* Corresponding authors.
E-mail addresses: mcm@swjtu.edu.cn (C. Ma), bcqsli@cityu.edu.hk (Q.S. Li).

https://doi.org/10.1016/j.engstruct.2018.11.007
Received 21 September 2017; Received in revised form 5 September 2018; Accepted 2 November 2018
0141-0296/ © 2018 Elsevier Ltd. All rights reserved.

Due to the above issues and the differences between the aerodynamic behavior of a bridge deck and that of the flat plate assumed by Sears, the Sears function may not be suitable for use as the aerodynamic admittance of a bridge deck. This may result in certain errors in the analysis of the dynamic response of long-span bridges under wind actions.

Since aerodynamic admittance was introduced into the buffeting analysis of bridges by Davenport [4], extensive studies have been conducted on the topic, such as Vickery and Clar [5], Holmes [6], Walshe and Wyatt [7], Xie and Gu [8], Jin and Xiang [9], Gu and Qin [10], Li and He [11], Li et al. [12], Li et al. [13], Yang et al. [14] and so on. However, the understanding of the complex fluid mechanisms involved in the interaction between a structure and turbulent wind is far from complete. A lack of deep investigations and sufficient experimental results may be another reason that studies of the aerodynamic admittance of bridge decks have not yet reached maturity. In fact, several researchers have drawn differing or even opposite conclusions. For example, Holmes [6], Walshe and Wyatt [7] and Hatanaka and Tanaka [15] observed that the aerodynamic admittance of a structure was greater than the Sears function, but Li and He found that the aerodynamic admittance of bridge decks was smaller than the Sears function, especially in low-frequency ranges.

Most of the previous studies of aerodynamic admittance were based on the “strip assumption” employed by Sears [2] and Davenport [4]. This assumption neglects the influence of the incident turbulence characteristics, particularly the turbulence length scale that is a representation of the average size of the most energetic turbulent eddies. In order to investigate the influence of different frequencies on the fluctuating wind lift “strip assumption”, Mugridge [16] presented the aerodynamic admittance formulation for a flat plate in terms of a function of two fluctuating wind wavelengths on the basis of a large amount of calculation:

$$|\phi(\widetilde{k}_1, \widetilde{k}_2)|^2 = \frac{1}{1 + 2\pi\widetilde{k}_1}\left(\frac{\widetilde{k}_1 + 2/\pi^2}{\widetilde{k}_1 + \widetilde{k}_2 + 2/\pi^2}\right) \tag{2}$$

where $\widetilde{k}_1 = \pi f_1 B/U$ and $\widetilde{k}_2 = \pi f_2 B/U$ represent the wavelength of the fluctuating wind and the degree of correlation along the spanwise direction and B is the width of the flat plate. Since this formula has 3-dimensional characteristic parameters, this kind of aerodynamic admittance is called the flat plate’s 3-dimensional aerodynamic admittance function (3D-AAF).

As the shapes of most bridge decks can be regarded as bluff bodies, their 3D aerodynamic admittance functions are generally complicated. Larose et al. [17] carried out a study on the 3D aerodynamic admittances of bridge sections and Jiang and Qiang [18] determined the 3D aerodynamic admittance of a thick plate using a taut strip model.

The wind flow in the Earth’s boundary layer is highly turbulent, and the wind loads acting on its structures are significantly influenced by the characteristics of the approaching turbulent flow. The turbulence characteristics of natural wind are usually identified according to two parameters: the intensity of the turbulent fluctuations of the wind (turbulence intensity) and their spectral distribution, which can also be partly defined by the average length of the turbulent gusts in the wind flow (turbulence scale). One of the most widely-used scales is the integral length scale, which is a representation of the average size of the most energetic turbulent eddies. The turbulence integral scale has been defined in several ways. It is often interpreted as the wavelength corresponding to the maximum normalized spectral density of the wind speed.

The effects of the free-stream turbulence intensity on the flows around bluff bodies have been the subject of a considerable amount of investigation. However, the effects of the turbulence integral scale on the aerodynamics of bluff bodies such as bridge decks have received relatively little attention. As reported by Li and Melbourne [19–21], the turbulence integral scale has a significant effect on the generation of peak and fluctuating wind pressures in the regions near leading edges on bluff bodies. There is therefore a need to conduct deep investigations of the effects of the turbulence integral scale on the aerodynamics of bridge decks.

Bridge spans have tended to become longer and longer as new materials and construction technologies have been developed. As the span increases, the natural frequencies generally decrease and a long-span bridge becomes more susceptible to resonant excitation by wind action. The buffeting analysis of long-span bridges therefore requires a more accurate aerodynamic admittance model to simulate the buffeting loads acting on bridges. In this paper, the aerodynamic admittances of the streamlined decks of long-span bridges are studied based on extensive pressure measurements made in wind tunnel tests. Furthermore, a 3D aerodynamic admittance model for such bridge decks is proposed. It is presented as a function of the characteristic size of a bridge deck and the turbulence integral length scale of the approaching wind flow.

2. Measurements of incident turbulence and fluctuating pressure

2.1. Turbulence simulation in wind tunnel tests

Two typical turbulent flow fields were simulated for the present wind tunnel tests and the associated turbulence generation arrangements are shown in Fig. 1. Grids were installed in Southwest Jiaotong University’s wind tunnel (Type: XNJD-2). The dimensions of the test section were 1.34 m × 1.54 m (width × height) and the wind speed ranged from 0.5 m/s to 20.0 m/s (turbulence intensity < 0.5%). Spires were installed in the wind tunnel (Type: XNJD-1). The dimensions of the test section were 3.6 m × 3.0 m (width × height) and the wind speed ranged from 0.5 m/s to 22.0 m/s (turbulence intensity < 0.5%).

The mean wind speed distributions and turbulence characteristic parameters were measured using a hotwire anemometer manufactured by DANTEC. Two X-probes were used to measure the longitudinal and vertical components of the wind velocity in the models’ positions without the models in place. Measurements were taken at 13 locations with 0.04 m intervals along the lateral direction in the horizontal plane to assess the incident turbulence correlations. The statistical features of the two kinds of turbulent flow are listed in Table 1 and the wind velocity spectral curves are presented in Fig. 2, in which the von Kármán spectrum [22] is also plotted for purposes of comparison. It has the form of

$$\frac{fS_u(f)}{\sigma_u^2} = \frac{4fL_u^x/U}{(1 + 70.8(fL_u^x/U)^2)^{5/6}}$$
$$\frac{fS_w(f)}{\sigma_w^2} = \frac{2(fL_w^x/U)(1 + 188.8(fL_w^x/U))^2}{(1 + 70.8(fL_w^x/U)^2)^{11/6}} \tag{3}$$

where $S_u(f)$ and $S_w(f)$ are the power spectral density of the longitudinal and vertical wind velocities, respectively; f is the frequency; σ_u and σ_w are respectively the standard deviations of the longitudinal and vertical fluctuating wind velocities; L_u^x and L_w^x are the integral length scales of the longitudinal and vertical fluctuating wind velocities; U is the mean wind speed in the longitudinal direction; u and w indicate the fluctuating wind velocities in the longitudinal and vertical directions, respectively.

The correlation coefficients of the two typical turbulent flow fields are shown in Fig. 3 and compared with those determined by the von Kármán model [22] which has the form of

$$R_u = \frac{2^{2/3}(r/a)^{1/3}K_{1/3}(r/a)}{\Gamma(1/3)}$$
$$R_w = \frac{2^{2/3}(r/a)^{1/3}\{K_{1/3}(r/a) - [r/(2a)]K_{-2/3}(r/a)\}}{\Gamma(1/3)} \tag{4}$$

where $a = 1.339L_i^x (i = u, w)$, r is the distance along the lateral direction, Γ is Gamma function and $K_{1/3}$ and $K_{-2/3}$ are modified Bessel functions of the second kind of order 1/3 and −2/3.

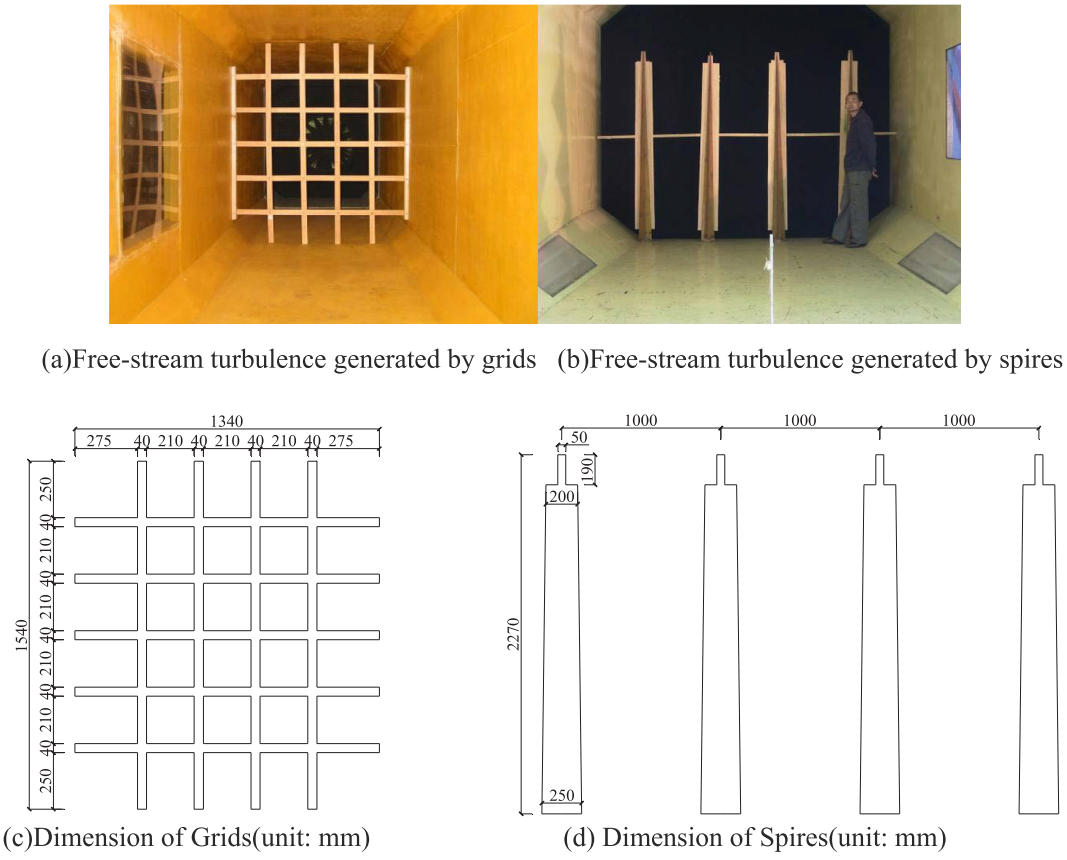

Fig. 1. Arrangements for generation of turbulent flow-fields.

Table 1
Turbulence characteristics of the wind fields simulated in the wind tunnel tests.

	I_u(%)	I_w(%)	L_u^x (m)	L_w^x (m)
Grid-generated turbulent field	7.71	7.59	0.091	0.04
Spire-generated turbulent field	12.1	10.1	0.49	0.41

2.2. Fluctuating pressure measurements of bridge section models

A plate model and two streamlined bridge decks models, shown in Fig. 4, were made for this study. The fluctuating pressures on the models were measured by a synchronous fluctuating pressure measurement system which could record pressure data from 60 pressure taps simultaneously. In the wind tunnel tests, two sections were measured in each recording run and about 30 pressure taps were used on each cross-section. One cross-section had fixed reference points while the other's were moved outside sequentially. The correlation characteristics of the buffeting forces between the two sections were thus measured. The measurement points (pressure taps) are shown in Fig. 4. The model installation details are shown in Fig. 5.

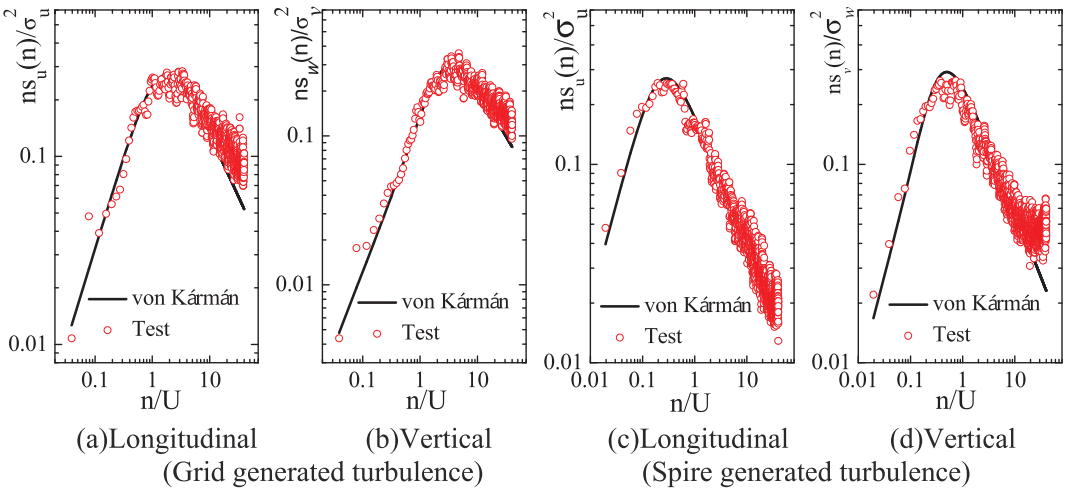

Fig. 2. Wind velocity spectra of the simulated turbulent flow-fields.

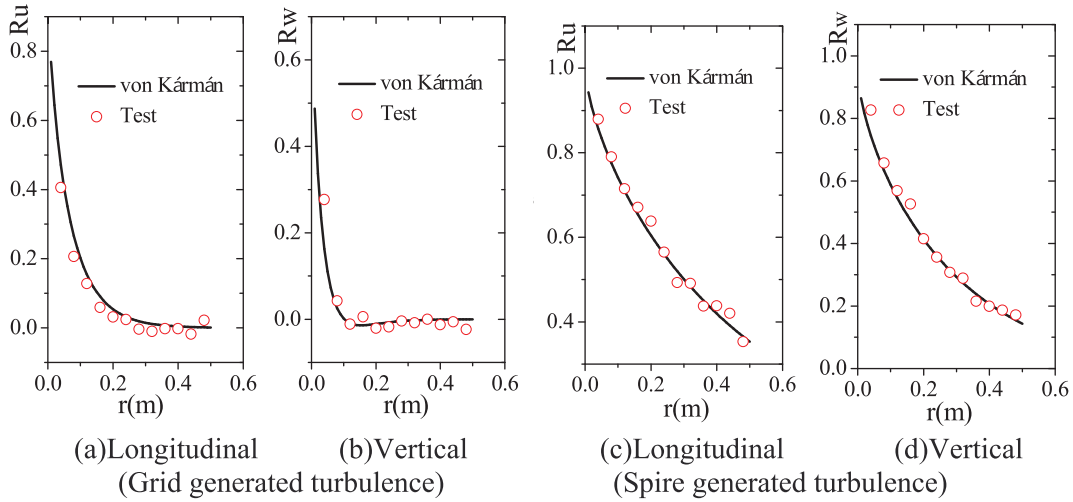

Fig. 3. Correlation coefficient of the simulated turbulent flow-fields.

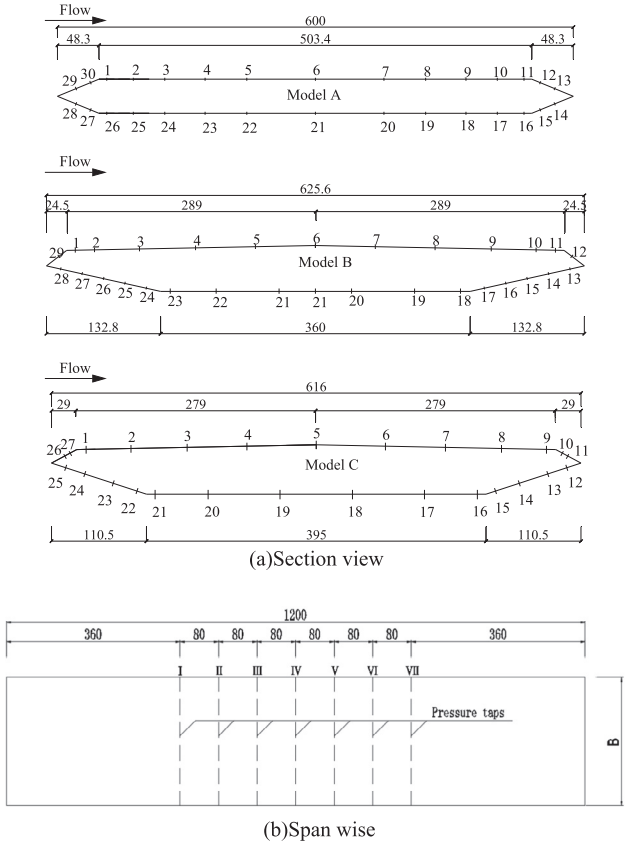

Fig. 4. Arrangements of pressure taps (unit: mm).

2.3. Distribution characteristics of the fluctuating pressures on the bridge deck models

The rms values of the fluctuating pressure coefficient C_{pri} at each pressure tap on the three models can be determined using the following equations:

$$C_{pri} = \frac{P_{ri}}{\frac{1}{2}\rho U^2}$$
$$P_{ri} = \sqrt{\frac{1}{N-1}\sum_{i=1}^{N}[P_i(t) - P_{ai}]^2} \quad (5)$$

where N is the length of the recorded data, ρ is the air density, $P_i(t)$ is the measured pressure data in the time series and P_{ai} is the average value of the pressure data at the i-th pressure tap.

As shown in Fig. 6, variations in the incident wind angle have a significant influence on the distribution of the fluctuating pressure coefficient, especially on the windward faces of the models. In the case of a negative approaching wind angle, the rms values measured by the pressure taps at the lower parts are relatively large. However, when the model is subjected to attacking wind with a positive angle, these values are small. It can be seen from the figure that the rms values on the windward sides are larger than those on the other sides of the same model. Regarding the differences between the fluctuating pressures of the three models, it can be found that the variations of the rms coefficients on Model A are less significant than those on the other models.

Some differences are observed between the rms fluctuating pressures measured in the two turbulent flow-fields. Under the spire-generated turbulent flow-field, the fluctuating pressures on the windward side are much greater than those on the leeward side, while under the grid-generated turbulent flow-field, the fluctuating pressures on both the windward side and the leeward side are distributed almost uniformly. This phenomenon can therefore be attributed to the difference of two wind fields. As shown in Table 1. The turbulence intensity and integral scale of the spire-generated turbulent flow-field are higher than those of the grid-generated turbulent flow-field.

2.4. Buffeting forces on the models

Based on the fluctuating pressure measurements, the buffeting lift forces and moments acting on the models can be determined using the following formulas:

$$L(t) = \sum_1^n P_i(t)dl\sin\alpha_i$$
$$M(t) = \sum_1^n P_i(t)dl\cos\alpha_i \cdot Y_i + \sum_1^n P_i(t)dl\sin\alpha_i \cdot X_i \quad (6)$$

where dl is the representative width of the i-th pressure tap, α_i is the angle between the normal direction of the plane where the pressure tap is located and axis x and X_i and Y_i are the distances between the i-th pressure tap and the torsional center of the model section along the x and y axes respectively.

The buffeting drag force of a model can be calculated using the measured fluctuating pressures. However, in the locations where most contributions to the drag force were made, there was not enough space to arrange more pressure taps to take the measurements. As a result, it was difficult to accurately determine the drag force. Therefore, only the lift force and moment will be discussed in the following parts.

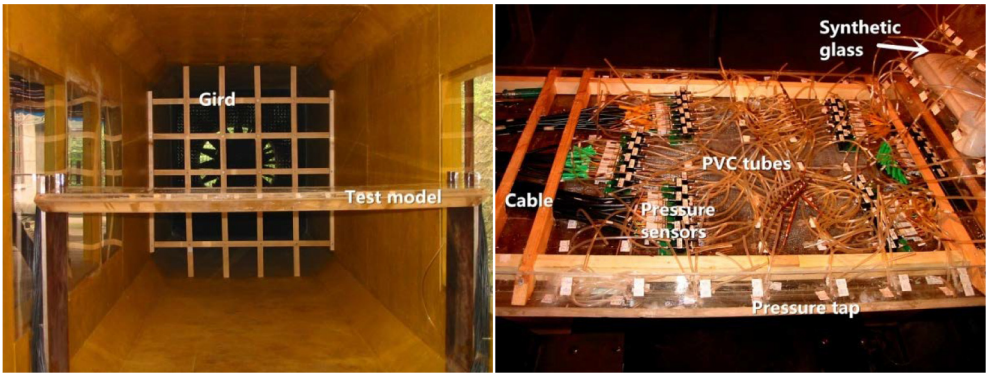

(a)Photo of a model in the wind tunnel (b)Pressure sensors inside a model

Fig. 5. Photos of the models and pressure sensors.

2.5. Coherence functions of the bridge decks along the spanwise direction

The coherence functions of the measured buffeting forces on the models can be obtained by

$$Coh(r,f)=\frac{S_r^C(f)}{S(f)} \tag{7}$$

where $S_r^C(f)$ is the co-spectrum of the buffeting forces between two crosswise sections which have a distance of r and $S(f)$ is the spectrum of the buffeting force.

Fig. 7 shows a comparison between the coherence functions of the incident turbulent wind velocity and the buffeting forces. As shown in Fig. 7, the coherences of the buffeting forces are found to be larger than those of the incident wind velocity. This suggests that conventional methods, which are generally based on the coherence values of the wind velocity, may result in the underestimation of the buffeting forces.

A formula for determining the coherence of the buffeting forces on the models is therefore needed. Roberts and Surry [23] derived the expression of the coherence function of the turbulence field based on the von Kármán model (Eq. (3)), which was extended by Irwin [24] to

$$\begin{aligned}
&Cu(r,f)=\frac{2^{1/6}}{\Gamma(5/6)}\left[\eta^{5/6}K_{5/6}(\eta)-\frac{\eta^{11/6}}{2}K_{1/6}(\eta)\right]\\
&Cw(r,f)=\frac{2^{1/6}}{\Gamma(5/6)}\left[\eta^{5/6}K_{5/6}(\eta)-\frac{\eta^{11/6}}{\theta}K_{1/6}(\eta)\right]\\
&\eta=\frac{r}{L_i^x}0.747\sqrt{1+70.8(fL_i^x/U)^2},\ (i=u,w)\\
&\theta=1+188.7(fL_i^x/U)^2,\ (i=u,w)
\end{aligned} \tag{8}$$

where f is the frequency, L_u^x and L_w^x are the integral length scales of the longitudinal and vertical fluctuating wind velocities, U is the mean wind speed, Γ is the Gamma function, $K_{5/6}$ and $K_{1/6}$ are modified Bessel functions of the second kind and r is the distance along the lateral direction.

An empirical formula for determining the coherence of the buffeting forces on the models, similar to the coherence function of the turbulence field, is obtained by fitting the measured results as follows:

$$C(r,f)=0.994\left[\eta^{5/6}K_{5/6}(\eta)-\frac{\eta^{11/6}}{\theta}K_{1/6}(\eta)\right] \tag{9a}$$

$$\begin{aligned}
&\eta=\frac{r}{aL_w^x}0.747\sqrt{1+70.8(afL_w^x/U)^b}\\
&\theta=1+(afL_w^x/U)^b
\end{aligned}$$

where a and b are the parameters that need to be fitted.

Parameters a and b can be obtained by fitting the test data using the least square method. The coherence function can be obtained as follows:

For lift force:

$$\begin{aligned}
&\eta=\frac{r}{4.32L_w^x}0.747\sqrt{1+70.8(4.32fL_w^x/U)^{1.15}}\\
&\theta=1+188.7(4.32fL_w^x/U)^{1.15}
\end{aligned} \tag{9b}$$

For moment:

$$\begin{aligned}
&\eta=\frac{r}{4.62L_w^x}0.747\sqrt{1+70.8(4.62fL_w^x/U)^{1.31}}\\
&\theta=1+188.7(4.62fL_w^x/U)^{1.31}
\end{aligned} \tag{9c}$$

It can also be found from Fig. 7 that the coherence of the buffeting forces is greater than that of the incident turbulence, and the coherence function along the spanwise direction is dependent on the turbulence integral length scale L_w and the reduced frequency.

3. Three-dimensional aerodynamic admittance function (3D-AAF) of the bridge decks

Based on the experimentally-determined spectra of the buffeting forces, the time-averaged aerodynamic force coefficients and the u and w spectra of the approaching wind velocity, the aerodynamic admittances of the models can be obtained using the following expressions [24].

$$\begin{aligned}
&|\chi_L(\omega)|^2=\frac{S_L(\omega)}{(\rho UB/2)^2\{4C_L^2S_u(\omega)+[C_L'+C_D]^2S_w(\omega)\}}\\
&|\chi_M(\omega)|^2=\frac{S_M(\omega)}{(\rho UB^2/2)^2\{4C_M^2S_u(\omega)+C_M'^2S_w(\omega)\}}
\end{aligned} \tag{9}$$

where $\omega=2\pi f$, $S_L(\omega)$ and $S_M(\omega)$ are the spectra of the lift force and moment, respectively; $S_u(\omega)$ and $S_w(\omega)$ are the spectra of the longitudinal wind speed and vertical wind speed, respectively; U is the mean wind speed in the longitudinal direction, ρ is the density of the air, B is the width of the model, C_D, C_L and C_M are the time-averaged drag coefficient, lift coefficient and moment coefficient, respectively and C_L', C_M' are the slopes of the time-averaged lift and moment coefficients as listed in Table 2.

The aerodynamic admittance functions of model A are shown in Fig. 8. It can be seen from the figure that the Sears function obviously overestimates the aerodynamic admittances of the lift and moment, especially in low frequency ranges. It is also shown that the turbulence integral length scale affects the values of the aerodynamic admittances to a remarkable degree. In a wind field with a larger turbulence integral length scale, the aerodynamic admittance of model A has a larger value.

The Mugridge function [15] can provide more reasonable aerodynamic admittance results for model A than those obtained using the Sears function. This is due to the fact that the Mugridge function takes the aerodynamic spatial characteristics into account. However, the measured values of the aerodynamic admittances are larger than those determined by the Mugridge function because model A is not an ideal

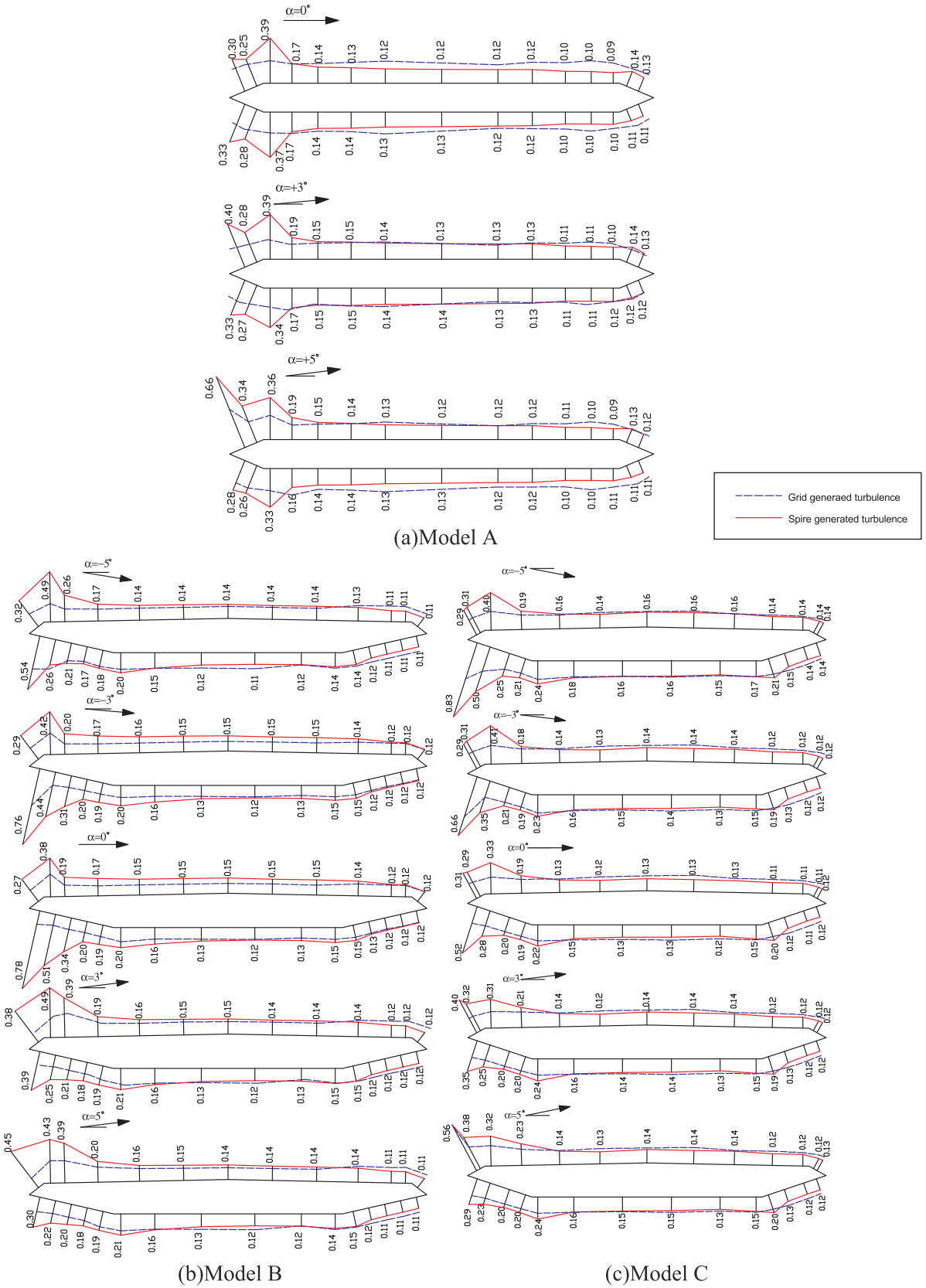

Fig. 6. Distributions of rms pressure coefficients on the three models.

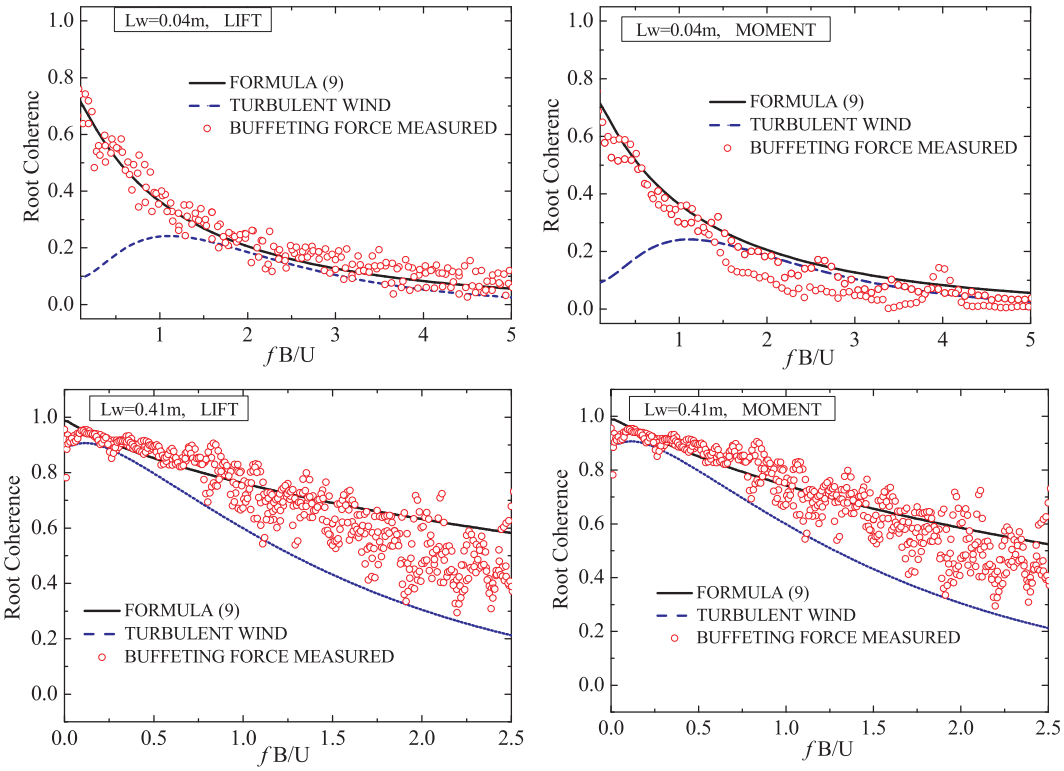

Fig. 7. Comparisons between the measured and calculated coherences of the buffeting forces with those of the incident wind for model A (the distance along the span is $r = 0.08$ m).

Table 2
Parameters of the models and related aerodynamic coefficients.

	B (m)	ρ (kg/m^3)	C_L	C_M	C'_L	C'_M
Model A	0.600	1.225	0.016	0.009	5.144	0.906
Model B	0.616	1.225	−0.226	0.021	5.302	1.305
Model C	0.626	1.225	−0.273	0.022	4.984	1.177

plate as the Mugridge function assumes.

3.1. Correlation coefficient of fluctuating pressures in crosswise sections

It is often believed that the aerodynamic admittance of a real bridge deck should be between 1 and the value determined by the Sears function. However, the present experimental results indicate that, in a low-frequency range, the aerodynamic admittance of a bridge deck is far lower than indicated by the Sears function. In order to explain this phenomenon, the correlation coefficients between the pressure tap ① and other measurement points on model A are presented in Fig. 9. It is obvious that the fluctuating pressures in a crosswise section are not completely correlated.

The assumption involved in the Sears function is that the turbulence integral scale is infinitely large in size compared to the characteristic length of the model concerned, which is to say that the correlation coefficient of the fluctuating pressures on the model is 1, meaning complete correlation. In fact, the turbulence integral scale is not infinitely larger and is usually in the same order as the characteristic length of a real structure. Therefore, the assumption does not actually hold in the cases of bridges. Fig. 9 demonstrates that the fluctuating pressures on a bridge section are not actually completely correlated and the correlation coefficient of the fluctuating pressure on a crosswise section is a function of the characteristic size of the bridge deck and the turbulence integral length scale, namely L_w/B. In other words, the wind-induced pressures are affected by the incident flow characteristics and the structural shape or dimensions. The actual buffeting force on a section is lower than that under the assumption of complete correlation; therefore, the aerodynamic admittance is lower than determined by the Sears function.

The correlation coefficients of the fluctuating pressures between the measurement point ① and other pressure taps on Model B and Model C are also shown in Fig. 9 and display similar distributions to those of Model A.

3.2. 3D-AAF of bridge decks

Since the turbulence integral length scale is generally not far greater than the characteristic size of a typical bridge deck, the Sears function was found to yield larger aerodynamic admittance values for bridge decks in low-frequency ranges. In fact, a suitable bridge deck aerodynamic admittance should be able to generate reasonable results for the following coherences:

(a) The coherence of the fluctuating pressures in a crosswise section;
(b) The coherence of the buffeting forces on different sections along the span direction.

Coherence (a) actually represents two-dimensional (2D) correlation information for a crosswise section, while (b) corresponds to that of the buffeting forces along the spanwise direction. The information regarding these two coherences represents the spatial characteristics of the aerodynamic forces on a whole structure. For a bridge deck, the associated aerodynamic admittances should adequately reflect these two aspects. Based on the above discussion, the correlation coefficient of the fluctuating pressure in a crosswise section is believed to be dependent on the turbulence integral scale and the characteristic size of a structure. Therefore, an accurate aerodynamic admittance is not only a function of the reduced frequency fB/U, but also of the turbulent integral scale and the characteristic size of a structure. The coherency of the buffeting forces along the spanwise direction should also depend on

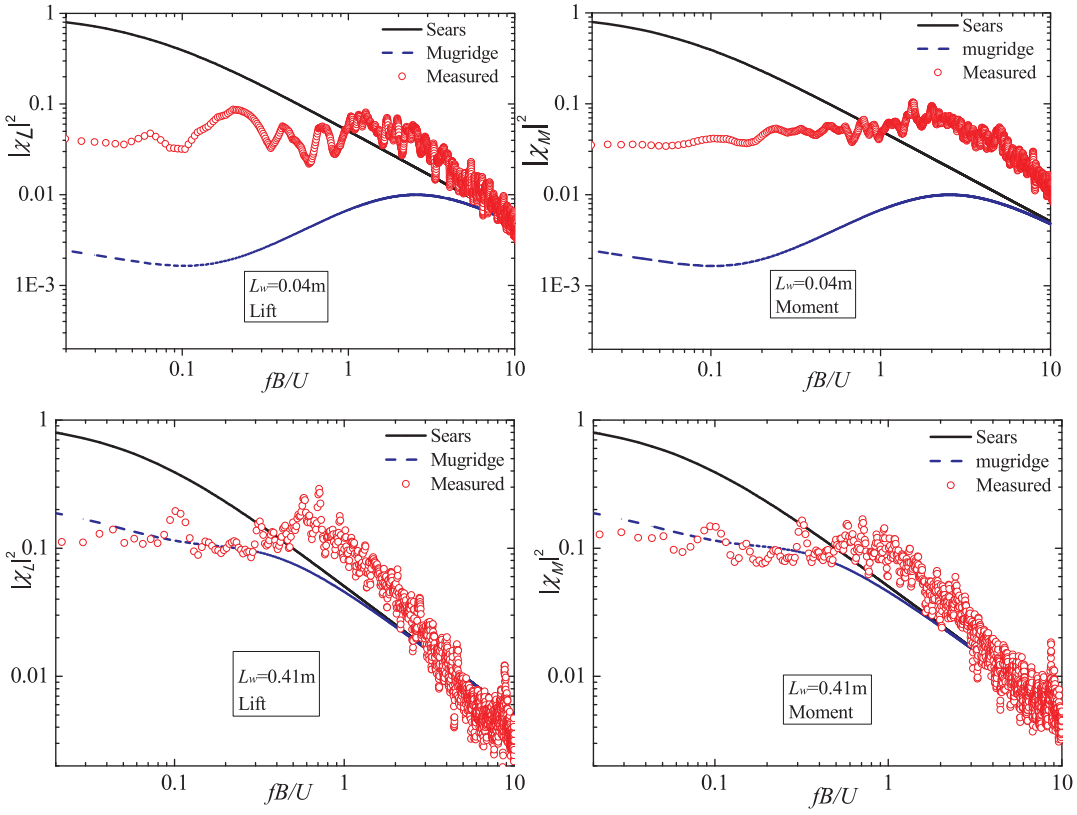

Fig. 8. Comparisons between the measured admittances of Model A and those obtained using the Mugridge function and the Sears function.

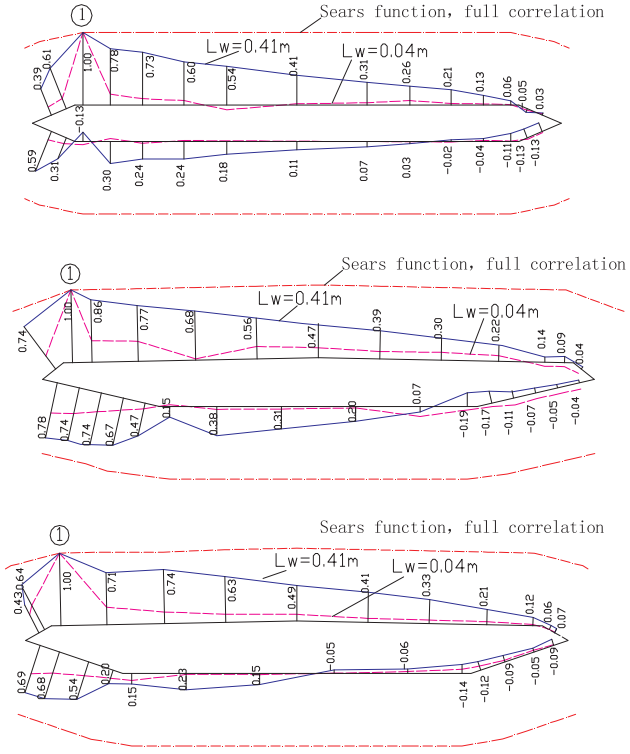

Fig. 9. Correlation coefficient of fluctuating pressures.

the turbulence integral length scale. Based on these analyses, a three-dimensional aerodynamic admittance function (3D-AAF) for streamlined bridge decks is proposed as follows:

$$|\chi_{L,M}(f_r, L_w/B)|^2 = \frac{\gamma}{1+\beta f_r^2} \tag{10}$$

where

$$f_r = fB/U,\ \gamma = a(L_w/B)^{0.5}(1+f_r^b),\ \beta = c(L_w/B)^{0.5}$$

Parameters a, b, and c can be obtained by fitting the model test data using the least square method. Table 3 lists the parameters using Eq. (4) to fit the model test data in the turbulent spire-generated flow-field in which L_w = 0.41 m, and Fig. 10 shows the fitted curves using this turbulence integral length scale value. The 3D-AAF model proposed in this paper is found to appropriately describe the aerodynamic admittances of the bridge decks. For the sake of verification, Fig. 11 shows the curves of the 3D-AAF using the same parameters and measured data as in the case of the turbulence integral length scale L_w = 0.04 m, which also demonstrates that the results determined by the proposed formula are in good agreement with those of the wind tunnel tests.

It is worth noting that the 3D AAF proposed in this paper has two application conditions: (i) Large-span streamlined box girder bridges under continuous turbulence. (ii) The integral scale of turbulence is the same order as the characteristic size of the bridge section.

Table 3
Parameters in the 3D-AAF determined by fitting the experimental data.

Model	Lift			Moment		
	a	b	c	a	b	c
A	0.1452	0.8023	1.795	0.1143	0.7665	1.413
B	0.1483	0.5209	1.190	0.1343	0.971	1.619
C	0.1207	0.5827	1.386	0.0935	0.9081	1.625

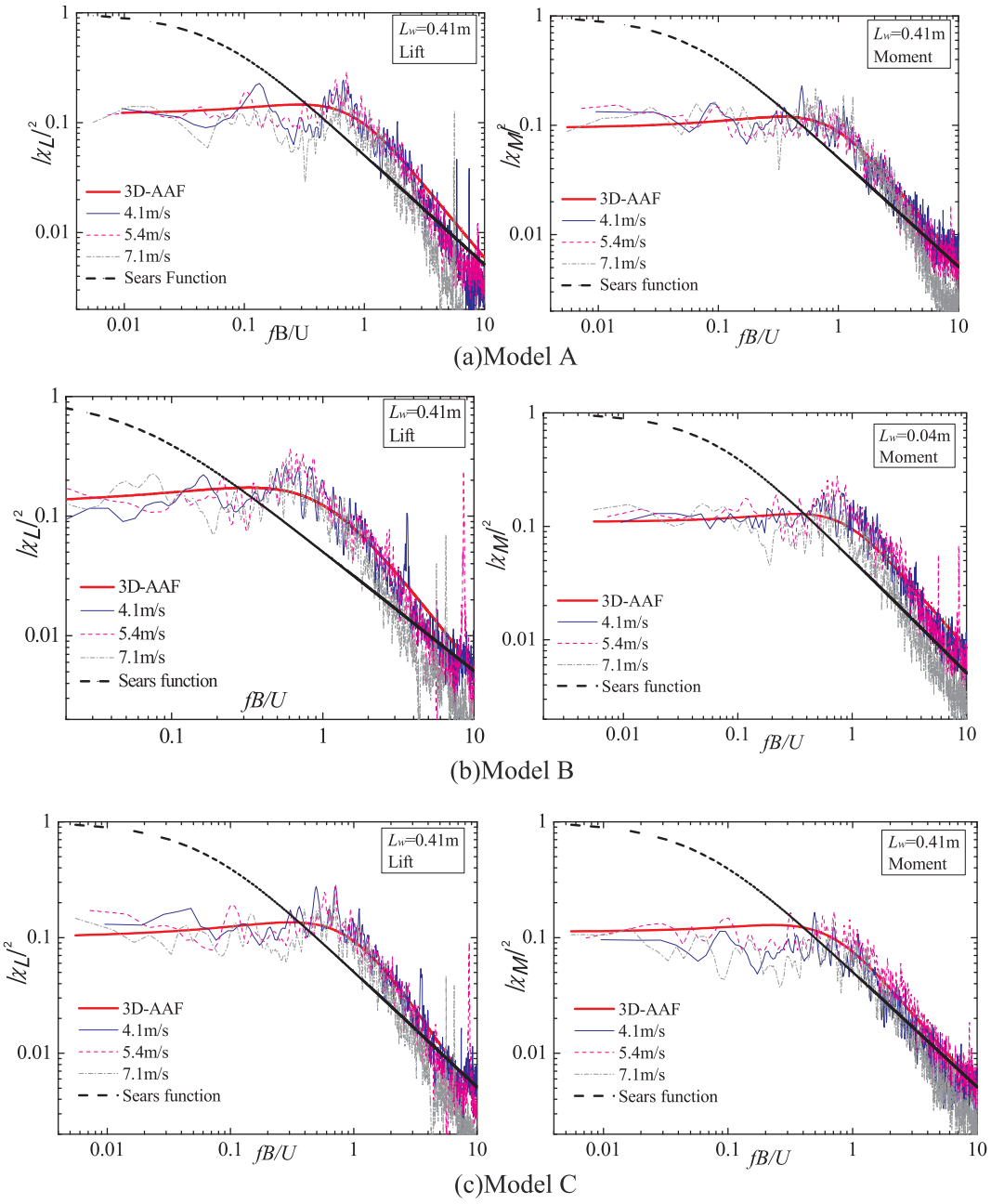

Fig. 10. Comparisons among the measured results, those of the proposed 3D-AAF and those of the Sears function for L_w = 0.41 m.

4. Conclusions

Extensive wind tunnel tests were conducted to measure the fluctuating pressures on the surfaces of three streamlined box bridge models in two turbulent flow-fields with different free-stream turbulence characteristic parameters. The distributions of fluctuating pressures on the models, the correlations of fluctuating pressures on crosswise sections and the coherences of the buffeting force along the spanwise direction of the models were presented and discussed. An empirical formula for determining the 3D aerodynamic admittances of streamlined bridge decks was proposed based on the results of the experimental data and analysis, which was verified to be an accurate aerodynamic admittance model for the simulation of the buffeting loads acting on bridges. Based on a detailed analysis of the measured data and comparative studies, conclusions are summarized as follows:

- The aerodynamic forces acting on bridges have strong 3D features; the existing aerodynamic admittance models based on the strip assumption may not be able to accurately simulate the buffeting forces on bridge decks.
- The aerodynamic admittance of a bridge deck is affected by the coherence of the fluctuating pressures on a crosswise section and the buffeting forces along the spanwise direction. Therefore, a reasonable 3D-AAF should be a function of reduced frequency L_w and structural characteristic width B.
- In low-frequency range, the aerodynamic admittances of a bridge deck are lower than those determined by the Sears function. Since most of a large-span bridge's buffeting responses are contributed by low-frequency components, the Sears function and other existing models may overestimate the buffeting responses.
- The coherences of buffeting forces were found to be larger than those of the incident wind velocity in the vertical direction. This suggests that the conventional methods generally based on the coherence values of such wind velocity may result in the

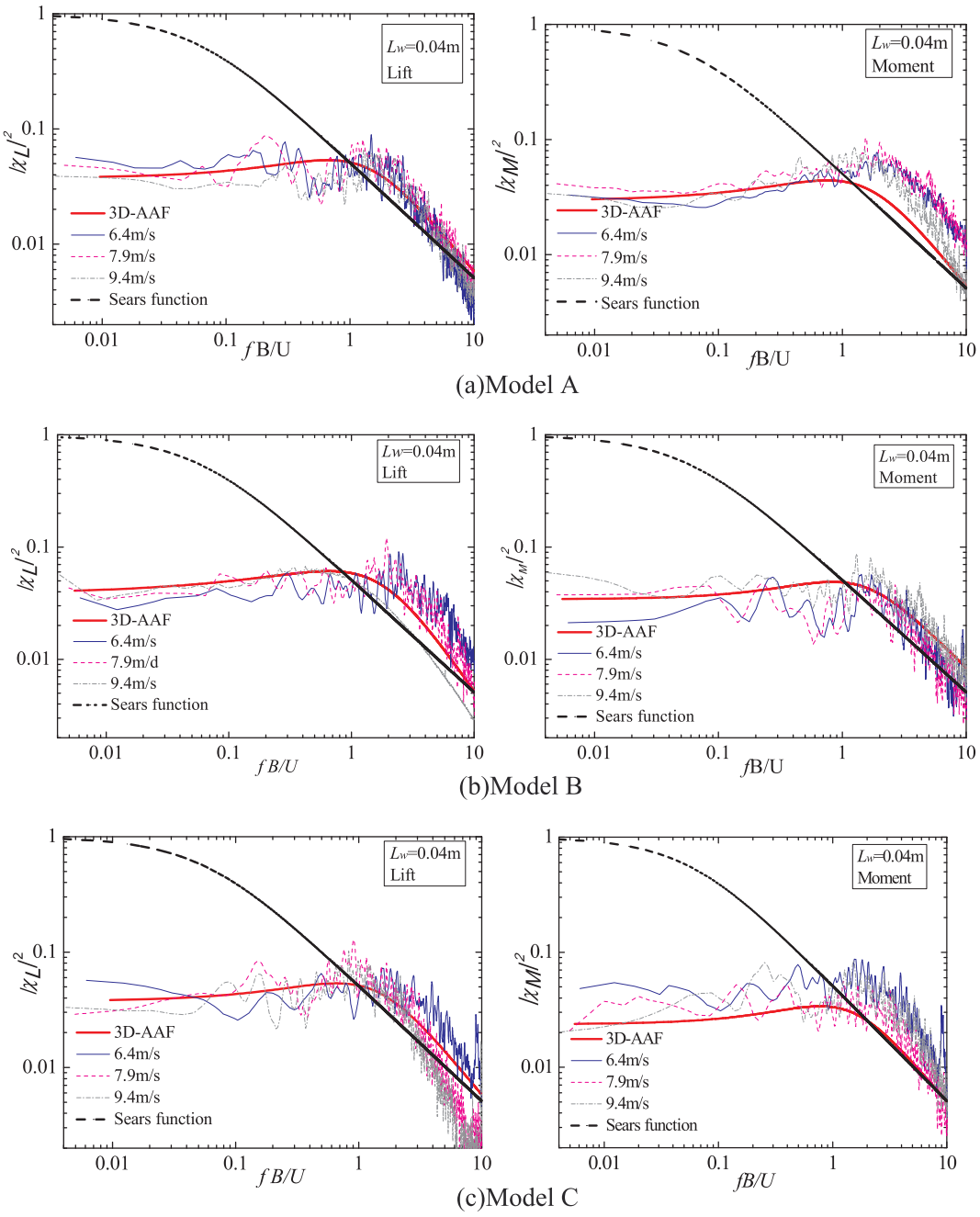

Fig. 11. Comparisons among the measured results, those of the proposed 3D-AAF and those of the Sears function for L_w = 0.04 m.

underestimation of the buffeting forces.

A 3D AAF and an empirical formula for the coherence of the buffeting forces on streamlined box bridge decks are established in this paper. The disadvantages of using the Sears function as the AAF of streamlined box bridge decks in the traditional algorithm are also corrected. However, due to the complexity of the geometric shapes of bridge decks, further and deeper studies of the aerodynamic admittance of different bridge sections, such as twin-box girders, truss beams and composite beams are required. Those deck forms are greatly different from streamlined box beams, and thus more work is needed to improve our understanding of the corresponding 3D AAF.

Acknowledgments

This project was supported by the National Natural Science Foundation of China (Grant number 51778545).

Appendix A. Supplementary material

Supplementary data to this article can be found online at https://doi.org/10.1016/j.engstruct.2018.11.007.

References

[1] Von Kármán T, Sears WR. Airfoil theory for non-uniform motion. J Aeronaut Sci 1938;10:379–90.
[2] Sears WR. Some aspects of non-stationary airfoil theory and its practical application. J Aeronaut Sci 1941;8(3):104–8.
[3] Liepmann HW. On the application of statistical concepts to the buffeting problem. J. Aeronautical Sci 1952;19(12):793–800.
[4] Davenport AG. The application of statistical concepts to the wind loading of structures. Proc ICE 1961;19(2):449–72.
[5] Vickery BJ, Clar AWK. Lift of across-wind response of tapered stacks. J Struct Div,

ASCE 1972;98(1):1–20.
[6] Holmes JD. Prediction of the response of a cable stayed bridge to turbulence. In: 4th international conference of wind effects on building and structures; 1975. p. 187–97.
[7] Walshe DE, Wyatt TA. Measurement and application of the aerodynamic admittance function for a box-girder bridge. In: 6th international conference on wind engineering; 1983. p. 211–22.
[8] Xie J, Gu M, Savage, et al. Identification of the aerodynamic admittance functions for bridge road decks. In: 2nd Asia-Pacific symposium on wind engineering; 1989. p. 618–28.
[9] Jin XH, Xiang HF. Identification of flat-plate aerodynamic admittance. J Tongji Univ 2003;31(10):1168–72.
[10] Gu M, Qin XR. Direct identification of flutter derivatives and aerodynamic admittances of bridge decks. Eng Struct 2004;26:2161–72.
[11] Li MS, He DX. Aerodynamic admittance of airfoil and bluff bodies. Acta Aerodyn Sinaca 2005;23(3):374–7.
[12] Li SP, Li MS, Ma CM. Buffeting analysis of long span bridge under skew wind in frequency domain. In: 8rd APCWE; 2013.
[13] Li SP, Li MS, Liao HL. The lift on an aerofoil in grid-generated turbulence. J Fluid Mech 2015;771:16–35.
[14] Yang Y, Li MS, Ma CM. Experimental investigation on the unsteady lift of an airfoil in a sinusoidal streamwise gust. Phys Fluids 2017;29(5):284.
[15] Hatanaka A, Tanaka H. Aerodynamic admittance functions of rectangular cylinders. J Wind Eng Ind Aerodyn 2008;96(6–7):945–53.
[16] Mugridge BD. Gust loading on a thin aerofoil. Aeronaut Quart 1971;22(4):301–10.
[17] Larose GL, Tanaka H, Gimsing NJ. Direct measurements of buffeting wind forces on bridge decks. J Wind Eng Ind Aerodyn 1998;74–76:809–18.
[18] Jiang YL, Qiang SZ. Experiment study on aerodynamic admittance function of thin plate. Exp Meas Fluid Mech 2001;15(4):26–9.
[19] Li QS, Melbourne WH. An experimental investigation of the effects of free-stream turbulence on streamwise surface pressures in separated and reattaching flows. J Wind Eng Ind Aerodyn 1995;51–52:313–23.
[20] Li QS, Melbourne WH. The effects of large scale turbulence on pressure fluctuations in separated and reattaching flows. J Wind Eng Ind Aerodyn 1999;83:159–69.
[21] Li QS, Melbourne WH. Turbulence effects on surface pressures of rectangular cylinders. Wind Struct 1999;2(4):253–66.
[22] Von Kármán T. Progress in the statistical theory of turbulence. Proc Natl Acad Sci 1948;34(11):530–9.
[23] Roberts JB, Surry D. Coherence of grid generated turbulence. Proc Am Soc Civ Eng J Eng Mech Div 1973.
[24] Chen ZQ, Xiang HF. Wind engineering of bridge. China: China Communications Press; 2005.